

# Impact of CYP3A offenders on ibrutinib exposure in individuals in good health

<sup>1</sup>DR.S.KUSUMAKUMARI,<sup>2</sup>DR.M.SPURTHIMITHRA,<sup>3</sup> DR C.RENUKATEJASWINI,  
<sup>4</sup>DR R SRIRAM,<sup>5</sup>S SAHEENA BEGUM,<sup>6</sup>E. HONEY

Department of Pharmacology, Dr K.V Subba Reddy Institute of Pharmacy

## Abstract

A number of B-cell malignancies have been successfully treated with ibrutinib (PCI-32765), a strong covalent inhibitor of Bruton's tyrosine kinase. The impact of co-administration of CYP3A perpetrators with ibrutinib was studied in healthy persons because to the significant function of CYP3A in the metabolism of ibrutinib. Both alone and in combination with ketoconazole (400 mg q.d. in Study 1), rifampin (600 mg q.d. in Study 2), grapefruit juice (GFJ, Study 3), and ibrutinib (120 mg in Study 1 fasting, 560 mg in Studies 2 fasted, and 3 nonfasted)) were administered. For safety reasons, CYP3A inhibitors were administered with lower dosages of ibrutinib [40 mg in Study 1 and 140 mg in Study 3]. While rifampin reduced ibrutinib exposure [C<sub>max</sub>: 13-fold; AUC<sub>last</sub>: 10-fold] under fasting conditions, ketoconazole enhanced DN exposure to ibrutinib [DN-AUC<sub>last</sub>: 24-fold; DN-C<sub>max</sub>: 29-fold]. Most likely by inhibition of intestinal CYP3A, GFJ produced a substantial rise under nonfasted conditions [DN-C<sub>max</sub>: 3.5-fold; DN-AUC: 2.2-fold]. The relationship seems to focus mostly on first-pass extraction while CYP offenders had little effect on half-life. Tolerance to all treatments was low.

Medical terms such as DDI, GFJ, LC-MS/MS, PBPK, and AE stand for adverse events, B-cell antigen receptor, Bruton's tyrosine kinase, and liquid chromatography tandem mass spectroscopy, respectively.

## Introduction

Tumorigenesis in most B-cell malignancies is thought to rely on B-cell antigen receptor (BCR) signaling. According to Fuentes-Panana et al. (2004) and Advani et al. (2013), normal B cells undergo antigen stimulation, which triggers the dimerization

of BCR and sets off a signaling cascade. This cascade affects several cellular activities, such as proliferation, differentiation, apoptosis, and survival. One potential therapeutic target in human cancers is Bruton's tyrosine kinase (BTK), an essential terminal kinase enzyme in the BCR signaling cascade. In addition to its involvement in the development, maintenance, and progression of adult B-cell lymphoproliferative disorders, this downstream signal transduction protein is essential for B-cell adhesion, chemotaxis, and trafficking (Kuppers 2005).

Patients with chronic lymphocytic leukemia and mantle cell lymphoma who have received at least one prior therapy can now take Ibrutinib, an orally active, BTK-targeting inhibitor (PCI-32765). This makes Ibrutinib the first covalent inhibitor of BTK to advance into human clinical trials. It

forms a stable covalent bond with cysteine-481 on the active site of BTK and irreversibly inhibits BTK phosphorylation on Tyr223, impairing BCR signaling, and disrupting the proliferation and survival of malignant B-cells (IC<sub>50</sub>: 0.39 nM) (Honigberg et al. 2010). Ibrutinib is almost exclusively metabolized by cytochrome P450 (CYP) CYP3A. Absolute oral bioavailability (*F*) is low, ranging from 3.9% in the fasted state to 8.4% following a standard breakfast without grapefruit juice (GFJ) and 15.9% with GFJ (de Vries et al. 2015). A major metabolite of ibrutinib, PCI-45227, is a dihydrodiol metabolite that displays reversible binding with an inhibitory activity toward BTK approximately 15 times lower than that of ibrutinib (Parmar et al. 2014).

Ibrutinib has a mean peak plasma concentration observed at 1–2 h after administration. The mean terminal half-life is 4–13 h, with minimum drug accumulation after repeated dosing (<twofold)

(Advani et al. 2013; Byrd et al. 2013; Imbruvica<sup>TM</sup>, 2014). Population pharmacokinetic (PK) analysis indicated that ibrutinib clearance is independent of age (Marostica et al. 2015).

Multiple medications are administered in conjunction with ibrutinib for concurrent diseases including those for opportunistic infections. Given the prominent role of CYP3A in ibrutinib metabolism, drug–drug interactions (DDIs) that affect ibrutinib exposure and its metabolites, may occur when coadministered with potent CYP3A inhibitors or inducers. It is thus essential to understand the PK profile of ibrutinib when interacting with the CYP enzyme system, which can affect drug metabolism and clearance as well as, alter their safety and efficacy profile and/or of their active metabolites.

This paper discusses results from three phase 1 studies which were undertaken to obtain a comprehensive understanding of DDI between ibrutinib and CYP3A perpetrators ketoconazole (strong inhibitor) (Study 1), rifampin (strong inducer) (Study 2), and single-strength GFJ (classified as a moderate inhibitor, specific for intestinal CYP3A) (Study 3) and their effect on ibrutinib exposure. Because it became clear during clinical development that food by itself significantly increases the relative bioavailability, Study 3 was performed in nonfasted condition. In this way, the CYP3A DDI could be assessed under more relevant conditions, and data from both fasted and non-fasted condition could be used in building a robust physiologically based pharmacokinetic (PBPK) model.

## Materials and methods

### Study population

Healthy participants (nonsmokers) aged 18–55 years (inclusive) with body mass index 18–30 kg/m<sup>2</sup> and body weight ≥50 kg were enrolled in all three studies. Study 1 enrolled only men, whereas studies 2 and 3 enrolled both men and women.

Participants with evidence of any clinically significant medical illness that could interfere with interpretation of study results or other abnormalities in physical examination, clinical laboratory parameters, vital signs, or ECG abnormalities etc. detected at screening, were

excluded from all three studies. Women were required to be post-menopausal or surgically sterile. In all three studies, participants were to refrain from taking any over-the-counter or prescribed medications except acetaminophen (<3 g per day).

Protocols for each study were approved by an Independent Ethics Committee or Institutional Review Board at each study site and the studies were conducted in accordance with the ethical principles originating in the Declaration of Helsinki and in accordance with the ICH Good Clinical Practice guidelines, applicable regulatory requirements, and in compliance with the protocol. All participants provided written informed consent to participate in the studies.

### Study design and treatment

Studies 1 and 2 were sequential design dedicated DDI studies of ibrutinib with ketoconazole and rifampin, respectively, versus Study 3, which was a two-way cross-over DDI study with GFJ, combined with a formal absolute bioavailability study following single oral dose administration of ibrutinib in comparison with a single intravenous (i.v.) administration. All three studies were single center, and open-label.

Study 1 (clinicaltrials.gov identifier: NCT01626651) consisted of three phases: screening period (21 days), open-label treatment period (10 days), and follow-up period (10 2 days). Participants received ibrutinib (120 mg, oral) on day 1 followed by blood sampling for PK analysis upto 72 h. Ketoconazole (Tara Pharmaceuticals), 400 mg oral, was given once-daily (q.d.) from days 4 to 9 (except on day 7); on day 7 they received ibrutinib (40 mg, oral) in combination with ketoconazole (400 mg, oral) 1 h before ibrutinib dosing.

Study 2 (clinicaltrials.gov identifier: NCT01763021) consisted of screening period (21 days), open-label treatment period (14 days) and follow-up period (10 2 days). Participants received ibrutinib, 560 mg, oral, q.d. on day 1. Rifampin (VersaPharm) 600 mg oral, q.d. was given from days 4 to 13 (after the last ibrutinib sample collection for PK [over 72 h]). On day 11, a second single oral dose of ibrutinib 560 mg was administered, followed by

the blood sample collection over 72 h.

In studies 1 and 2, ibrutinib was administered after overnight fast; food was withheld for 4 h after ibrutinib administration on dosing days.

Study 3 (clinicaltrials.gov identifier: NCT01866033) consisted of screening period (21 days), open-label treatment period (treatment A, B and C) (19 days), and follow-up period (10–2 days). All participants received ibrutinib (560 mg) in treatment A and then randomized to either treatment B (ibrutinib [560 mg] administered 30 min after 240 mL of glucose in water) or treatment C (240 mL of GFJ [Albert Heijn pink] the evening before and 30 min before ibrutinib [140 mg]). In treatments B and C, participants had standard breakfast 30 min after ibrutinib dosing, as opposed to treatment A which was given in fasted condition. A single i.v. dose of 100  $\mu$ g  $^{13}\text{C}_6$  PCI-32765 was administered 2 h after each ibrutinib oral dose.

In all three studies, participants took ibrutinib with 240 mL of water and lunch and subsequent standard meals were provided 4 h after oral ibrutinib dosing. Participants remained seated throughout morning (from 30 min before dosing until after lunch), in order to minimize inter and intrasubject intestinal blood flow differences.

## Pharmacokinetic evaluations

### Sample collection

Blood samples for all studies were collected by direct venipuncture or through an indwelling peripheral venous heparin lock catheter into heparin collection tubes. Samples were centrifuged at approximately 4°C (15 min at 1300 g); plasma was stored at  $\leq -70^\circ\text{C}$ .

Blood samples for PK analysis were collected predose and 0.5, 1, 1.5, 2, 3, 4, 6, 8, 12, 16, 24, 48, and 72 h post-dose on days 1 and 7 (Study 1 and 3) and days 1 and 11 (Study 2) for quantification of ibrutinib and PCI-45227. Additional blood samples were collected 2 h after ketoconazole dosing on day 7 (1 h after ibrutinib dosing) (Study 1) and 2 h after rifampin dosing on day 11 (Study 2) for ketoconazole and rifampin measurement, respectively. In Study 2, samples were collected and analyzed for determination of 4-b-hydroxycholesterol concentration on day -1, 12 h after ibrutinib administration on day 11 and 14.

## Analytical methods

Plasma concentrations of ibrutinib, its metabolite, PCI-45227, ketoconazole, rifampin, and  $^{13}\text{C}_6$  ibrutinib, were determined using validated analytical liquid chromatography-tandem mass spectroscopy (LC-MS/MS) methods. Bioanalyses were conducted at Department of Bioanalysis, Janssen R&D and at Frontage Laboratories, Inc., Exton, PA.

Quantification range was 0.100–25.0 ng/mL for ibrutinib and PCI-45227 (Study 1 and 2) and 0.5–100 ng/mL (Study 3) (de Vries et al. 2015). Quantification range for  $^{13}\text{C}_6$  PCI-32765 was 2–1000 pg/mL (de Vries et al. 2015).

## Pharmacokinetic analysis

PK analyses were performed by noncompartmental methods using validated WinNonlin<sup>®</sup> software Version 5.2.1 (Certara USA, Inc. Princeton, NJ) and Phoenix WinNonlin.

6.3. Key PK parameters included maximum observed plasma concentration ( $C_{\text{max}}$ ), time to reach maximum observed plasma concentration ( $t_{\text{max}}$ ), elimination half-life associated with terminal slope ( $k_z$ ) of the semilogarithmic drug concentration-time curve ( $t_{1/2k}$ ), area under the plasma concentration-time curve (AUC) from time 0 to 24 h ( $\text{AUC}_{24}$ ), AUC from time 0 to time of the last quantifiable concentration ( $\text{AUC}_{\text{last}}$ ), AUC from time 0 to infinity ( $\text{AUC}_{\infty}$ ) and metabolite/parent ratios. In Study 1, apparent total clearance of drug after extravascular administration ( $\text{CL}/F$ ), and apparent volume of distribution based on the terminal phase ( $V_{d_z}$ ) were also estimated. Additionally, in Study 3, absolute bioavailability ( $F$ ) and total clearance of drug after i.v. administration ( $\text{CL}$ ) were also estimated.

## Safety evaluations

Safety evaluations included assessments of treatment-related adverse events (AE), vital signs, 12-lead electrocardiograms, clinical laboratory tests, and physical examinations. The AE severity was graded according to the National Cancer Institute - Common Terminology Criteria for Adverse Events (NCI-CTCAE) grading system version 4.03.

## Analysis sets

Participants who had estimations of PK parameters of ibrutinib for both periods (ibrutinib administered alone and in combination with CYP3A perpetrators) were included in PK analysis set for statistical comparison. Participants who received at least one dose of study medication were included in safety analysis set.

## Sample size determination

For all three studies, sample size determinations were based on statistical estimation. A sample size is considered adequate if the point

## Pharmacokinetic results

*Study 1: effect of ketoconazole on pharmacokinetics of ibrutinib and its metabolite*

Following coadministration of ibrutinib with ketoconazole under fasted condition, mean DN\_ $C_{\max}$  (dose normalized to 120 mg) of ibrutinib increased from 11.8 to 325 ng/mL and mean DN\_ $AUC_{\text{last}}$  increased from 71.4 to 1599 ng·h/ mL (Fig. 1A). Although dose proportionality was not formally tested for ibrutinib, no deviations from linearity were observed neither in the Phase I escalating dose study nor population PK study (imbruvica<sup>TM</sup> 2014; Marostica et al. 2015), thus justifying the dose-normalization of ibrutinib exposure in this study. Intersubject variability in ibrutinib+ketoconazole treated participants for both  $C_{\max}$  and  $AUC_{\text{last}}$  were >50% following ibrutinib administration alone and approximately 40% when coadministered with ketoconazole. The  $V_d/F$  and  $CL/F$  were both lower following ibrutinib + ketoconazole compared with ibrutinib alone ( $V_d/F$ : 885 L vs. 19049 L;  $CL/F$ : 92.0 L/h vs. 2014 L/h, whereas there was no change in mean  $t_{\max}$  (2.00 h vs. 1.75 h) and  $t_{1/2}$  (6.32 h vs. 8.20 h) (Table S1). On the other hand, dose-normalized PCI-45227 exposure was lower following coadministration with ketoconazole compared with ibrutinib administration alone (Fig. 1B). The DN\_ $C_{\max}$  was 2.6 times lower (11.1 ng/mL

33.7 (8.8) 41.1 (11.6) 46.4 (8.1)

78.0 (7.4) 77.6 (8.7) 70.0 (13.2)

26.1 (2.3) 26.4 (2.5) 23.5 (2.7)

374 ng·h/mL (Fig. 2B). Intersubject variability for both  $C_{\max}$  and  $AUC_{\text{last}}$  was greater than 30% following ibrutinib administration alone and greater than 20% following ibrutinib + rifampin. Similar to the parent, median  $t_{\max}$  of the metabolite was delayed following ibrutinib + rifampin coadministration compared with ibrutinib treatment alone (from 2.02 to 3.00 h). Terminal  $t_{1/2}$  trended shorter for the combination treatment. The GMR for  $C_{\max}$  and  $AUC_{\text{last}}$  was 7.94% and 10.44% (or a 13- and 10-fold decrease), respectively, for ibrutinib + rifampin compared with ibrutinib alone (Table 2). Metabolite to parent ratio

Table 2. Geometric mean ratio and the 90% CI of the combination treatment (studies 1, 2, and 3) over ibrutinib.

| Parameter                                    | Test treatment/reference treatment <sup>7</sup> | N   | Geometric mean | Ratio: (%) <sup>8</sup> | 90% CI (%) <sup>8</sup> | Intrasubject CV (%) |
|--|---|-----|----------------|-------------------------|-------------------------|---------------------|
| Ibrutinib                                    | +   |     |                |                         |                         |                     |
| Ketoconazole <sup>4</sup>                    | Ibrutinib                                       | +18 | 286            | 2854.5                  | 2397–3400               | 31                  |
| $C_{\max}$ (ng/mL) <sup>1,2</sup>            | Ketoconazole Ibrutinib                          | 18  | 10             |                         |                         |                     |
| $AUC_{24}$ (ng·h/mL) <sup>1,2</sup>          | Ibrutinib                                       | +18 | 1390           | 2480.1                  | 2002–3073               | 38                  |
|  | Ketoconazole Ibrutinib                          | 18  | 56             |                         |                         |                     |
| $AUC_{\text{last}}$ (ng·h/mL) <sup>1,2</sup> | Ibrutinib                                       | +18 | 1463           | 2392.8                  | 1901–3012               | 41                  |
|  | Ketoconazole Ibrutinib                          | 18  | 61             |                         |                         |                     |
| $AUC_{\infty}$ (ng·h/mL) <sup>1,2</sup>      | Ibrutinib                                       | +12 | 1860           | 2620.2                  | 1996–3440               | 39                  |
|  | Ketoconazole Ibrutinib                          | 12  | 71             |                         |                         |                     |
| Ibrutinib + Rifampin <sup>5</sup>            |   |     |                |                         |                         |                     |
| $C_{\max}$ (ng/mL) <sup>2</sup>              | Ibrutinib + Rifampin                            | 17  | 3              | 7.9                     | 6–12                    | 69                  |
|  | Ibrutinib                                       | 17  | 32             |                         |                         |                     |
| $AUC_{24h}$ (ng·h/mL) <sup>2</sup>           | Ibrutinib + Rifampin                            | 17  | 23             | 10.9                    | 8–15                    | 61                  |
|  | Ibrutinib                                       | 17  | 214            |                         |                         |                     |
| $AUC_{\text{last}}$ (ng·h/mL) <sup>2</sup>   | Ibrutinib + Rifampin                            | 17  | 28             | 10.4                    | 7–15                    | 62                  |
|  | Ibrutinib                                       | 17  | 267            |                         |                         |                     |
| $AUC_{\infty}$ (ng·h/mL) <sup>2</sup>        | Ibrutinib + Rifampin                            | 4   | 46             | 15.2                    | 5–46                    | 74                  |
|  | Ibrutinib                                       | 4   | 300            |                         |                         |                     |
| Ibrutinib                                    | +   |     |                |                         |                         |                     |
| Grapefruit Juice <sup>6</sup>                |   |     |                |                         |                         |                     |
| $C_{\max}$ (ng/mL) <sup>2,3</sup>            | Ibrutinib + GFJ                                 | 8   | 437            | 360.4                   | 269–483                 | 31                  |
|  | Ibrutinib                                       | 8   | 121            |                         |                         |                     |
| $AUC_{24}$ (ng·h/mL) <sup>2,3</sup>          | Ibrutinib + GFJ                                 | 7   | 1337           | 252.9                   | 219–293                 | 13                  |
|  | Ibrutinib                                       | 7   | 529            |                         |                         |                     |
| $AUC_{\text{last}}$ (ng·h/mL) <sup>2,3</sup> | Ibrutinib + GFJ                                 | 8   | 1236           | 210.2                   | 182–243                 | 15                  |
|  | Ibrutinib                                       | 8   | 588            |                         |                         |                     |
| $AUC_{\infty}$ (ng·h/mL) <sup>2,3</sup>      | Ibrutinib + GFJ                                 | 7   | 1378           | 214.5                   | 184–250                 | 14                  |
|  | Ibrutinib                                       | 7   | 643            |                         |                         |                     |

CV, coefficient of variation; GFJ, grapefruit juice.

<sup>1</sup>Parameter values were natural log (ln) transformed and dose normalized to 120 mg ibrutinib before analysis.<sup>2</sup>A mixed-effect model with treatment as a fixed effect and participant as a random effect was used. Parameter values were natural log (ln) transformed before analysis.<sup>3</sup>The oral ibrutinib with grapefruit juice treatment group was dose normalized to 560 mg.

<sup>4</sup>Ibrutinib: 40 mg and ketoconazole: 400 mg.

<sup>5</sup>Ibrutinib: 560 mg and rifampin: 600 mg.

<sup>6</sup>Ibrutinib: 560 mg and GFJ: 240 mL.

<sup>7</sup>Test Treatment: ibrutinib + ketoconazole/ibrutinib + rifampin/ibrutinib + grapefruit juice, Reference Treatment: ibrutinib.



for  $C_{\max}$  increased from 2.09 to 20.80, and the ratio for  $AUC_{\text{last}}$  increased from 3.10 to 15.50.

Plasma concentrations for rifampin on day 11, 2 h after drug intake ranged from 289 ng/mL to 18400 ng/mL (mean  $\pm$  SD = 9247  $\pm$  4957 ng/mL). Low concentration of 289 ng/mL did not adversely affect induction, as decrease in ibuprofen exposure on day 11 in this participant was comparable with that observed in other participants. Compared with predose values (39.9 [15.50] ng/mL), 4-b-hydroxycholesterol concentrations increased following multiple once-daily oral administrations of rifampin, providing evidence that sufficient induction of CYP3A had occurred when 560 mg ibuprofen (day 11) was administered after 1 week of rifampin 600 mg q.d., and that induction was maintained until the 72-h PK sample was collected on day 14 (day 11: 97.3 [29.4] ng/mL and day 14: 119 [39.6] ng/mL).

### Study 3: effect of GFJ on ibuprofen exposure

Pretreatment with GFJ increased ibuprofen concentrations in plasma.  $DN_{C_{\max}}$  of ibuprofen increased by 3.5-fold, whereas  $DN_{AUC}$  increased by 2.2-fold in presence of single-strength GFJ compared with oral administration of 560 mg ibuprofen without GFJ under nonfasted condition (Fig. 2C). On the other hand, the AUCs of ibuprofen following i.v. administration under nonfasted conditions with and without GFJ were the same. Mean  $C_{\max}$  was slightly higher with GFJ, but intrasubject variability was very high (84%) (Fig. 3).

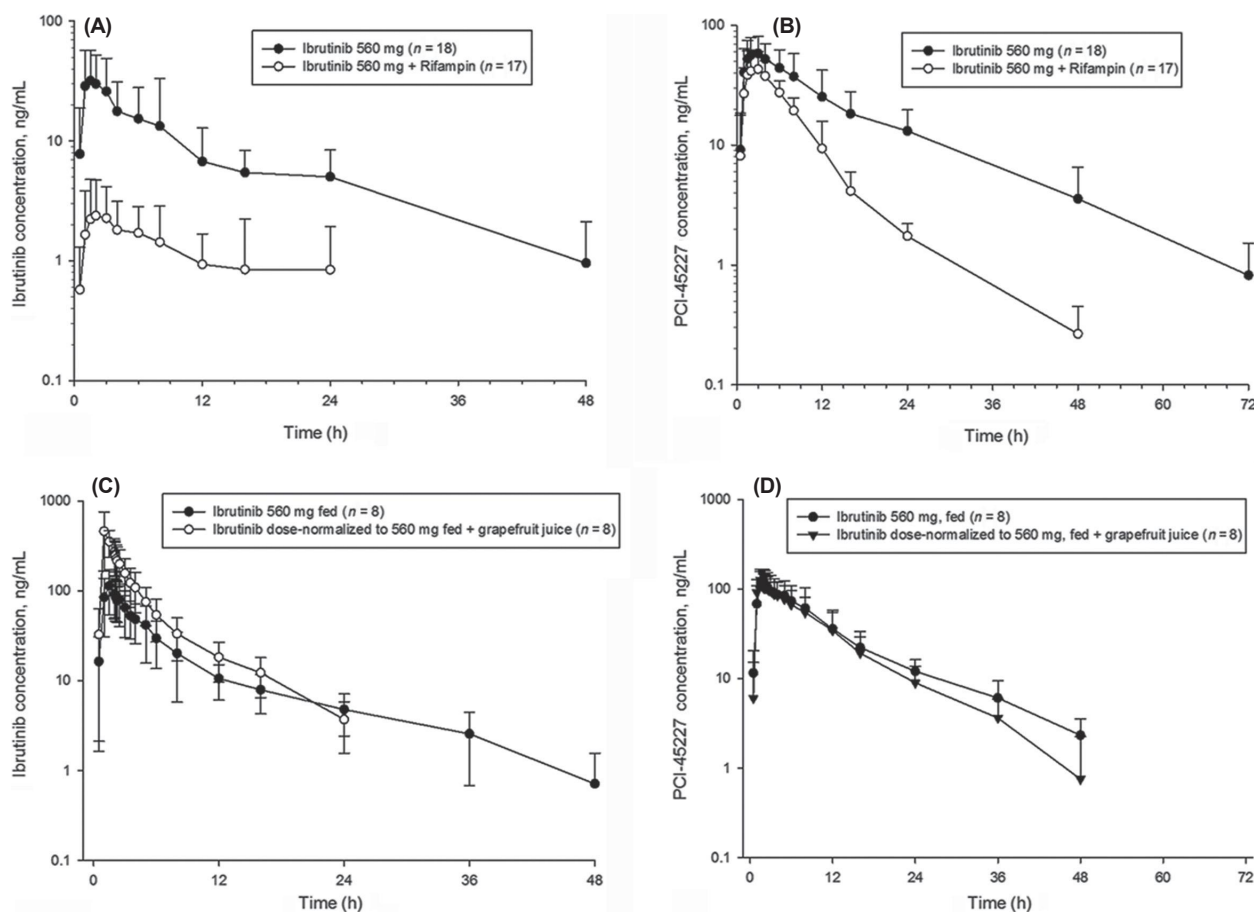


Figure 2. Mean (SD) logarithmic-linear plasma concentration-time profiles of ibuprofen (560 mg) and metabolite PCI-45227 in absence and presence of CYP perpetrators: Rifampin (600 mg) (A and B: fasted condition) Grapefruit Juice (C and D: nonfasted condition).



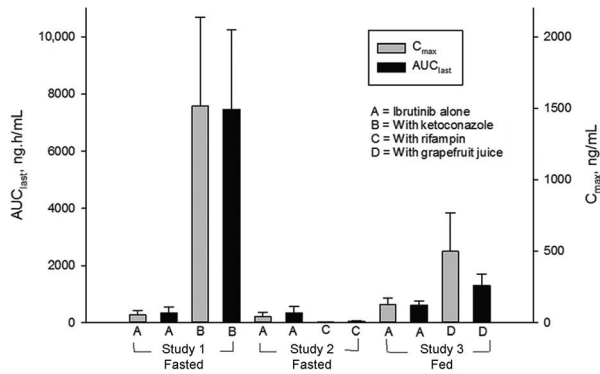


Figure 3. Mean (SD)  $AUC_{last}$  and  $C_{max}$  of ibrutinib following oral administration of ibrutinib alone and in combination with ketoconazole, rifampin, or grapefruit juice; data dose normalized to 560 mg.

There was no effect of GFJ on  $t_{max}$  of PCI-45227 (Fig. 2D). Dose-normalized PCI-45227 concentrations and AUCs following oral administration of ibrutinib with or without GFJ were comparable.  $C_{max}$  metabolite-to-parent ratio decreased from 1.03 to 0.32 with the addition of GFJ.

When ibrutinib was orally administered with GFJ, apparent clearance,  $CL/F$  and half-life both decreased by half;  $CL$  after i.v. administration, however, was unchanged with or without GFJ. The  $CL$  following i.v. administration under nonfasted condition was higher than that under fasted condition.

The magnitude of observed DDI was higher with higher baseline clearance. The higher the baseline  $CL/F$ , the larger the effect of ketoconazole. This trend was not observed clearly for the weaker (and intestine-specific) inhibitor GFJ, or for the inducer rifampin (Fig. 4).

### Safety

Treatments were generally well-tolerated in all three studies. In Study 1, only one (6%) participant reported  $\geq 1$  AE (musculoskeletal discomfort) after ibrutinib administration alone, and six participants (33%) reported  $\geq 1$  AE CYP3A Perpetrators and Ibrutinib Exposure

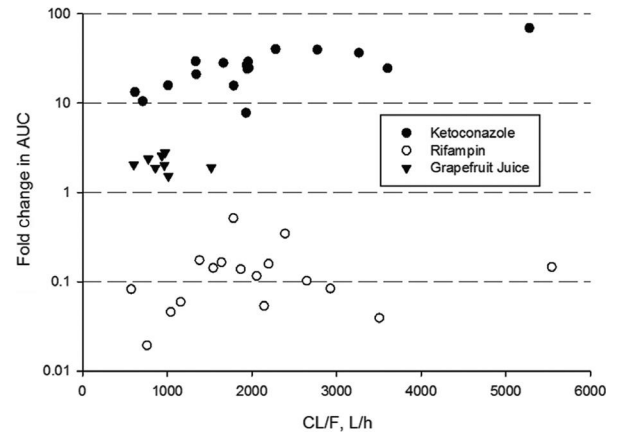


Figure 4. Fold-change in AUC versus baseline apparent clearance following oral administration of ibrutinib with ketoconazole or rifampin (both under fasted conditions) or with grapefruit juice (with standard meal).

Table 3. Summary of treatment-emergent adverse events (AE) seen in more than 10% of participants in any study (safety analysis set).

|   | Study 1 <sup>1</sup><br><i>n</i> = 18<br><i>n</i> (%) | Study 2 <sup>2</sup><br><i>n</i> = 18<br><i>n</i> (%) | Study 3 <sup>3</sup><br><i>n</i> = 8<br><i>n</i> (%) |
|---|---|---|--|
| Number of participants with treatment-emergent AE | 6 (33)  | 7 (39)  | 3 (38)   |
| Diarrhea  | —   | —   | 3 (38)   |
| Abdominal pain                                    | —   | —   | 3 (38)   |
| Dyspepsia   | —   | —   | 1 (13)   |
| Flatulence  | —   | —   | 1 (13)   |
| Vomiting  | —   | —   | 1 (13)   |
| Nausea  | —   | —   | 1 (13)   |
| Toothache   | —   | 2 (11)  | —  |
| Musculoskeletal discomfort                        | —   | 2 (11)  | —  |
| Back injury                                       | —   | —   | 1 (13)   |
| Epicondylitis                                     | —   | —   | 1 (13)   |
| Dizziness   | —   | —   | 2 (25)   |
| Headache  | 4 (22)  | 3 (17)  | 1 (13)   |
| Hyperventilation                                  | —   | —   | 1 (13)   |

<sup>1</sup>Study 1: ibrutinib + ketoconazole.

<sup>2</sup>Study 2: ibrutinib + rifampin.

<sup>3</sup>Study 3: ibrutinib + grapefruit juice.

following coadministration with ketoconazole. In Study 1, the most common AEs (>10%) following ibrutinib+ketoconazole coadministration were headache ( $n = 4$ , 22%), venipuncture-related hematoma and pain ( $n = 1$ , 6%), abdominal discomfort and dyspepsia ( $n = 2$ , 11%) (Table 3). All AEs were mild in severity (grade 1), limited in duration, and, resolved without medical intervention. In Study 2, 5 participants (28%) reported  $\geq 1$  AE after ibrutinib administration alone, compared with 22% ( $n = 4$ ) following combination therapy with rifampin. Most common AEs following treatment with ibrutinib alone were musculoskeletal discomfort ( $n = 2$ , 11%) and following ibrutinib+rifampin included toothache ( $n = 2$ , 11%) and headache ( $n = 3$ , 17%). All AE were of grade 1 intensity except for two participants who experienced grade

2 AEs (headache and morbilliform skin rash) following rifampin treatment. In Study 3, the most common AEs reported by >1 subject included abdominal pain, diarrhea, and dizziness. All events were grade 1 in severity except for grade 2 abdominal pain in one participant. There were no serious AEs, AEs leading to discontinuation or AEs that did not resolve at end of the study, reported in the three studies. There were no relevant changes in vital signs or 12-lead ECG, laboratory safety or changes in physical examination findings in any of the studies.

## Discussion

Ibrutinib is extensively metabolized by CYP3A and has low bioavailability due to extensive first-pass metabolism. Low bioavailability results in more variable PK and

potential variability in desired therapeutic response as well as undesirable adverse effects. Studies reported here were therefore designed to understand the DDI potential between ibrutinib and CYP3A perpetrators (ketoconazole, rifampin and GFJ) and their probable effects on ibrutinib bioavailability in healthy participants.

In line with in vitro data that showed 96% of microsomal clearance could be attributed to CYP3A4 (Scheers et al. 2015), CYP3A perpetrators had a major effect on ibrutinib exposure, without affecting the terminal half-life. There was an increase in ibrutinib concentration following coadministration with ketoconazole; intersubject variability was lower compared to ibrutinib alone, which can be explained by close to complete bioavailability in this situation. Though ketoconazole concentration was within the observed range, a low value observed in two participants may be due to the overexpression of CYP3A in these two participants. These values correlated with ibrutinib  $C_{max}$  and AUC that were approximately 80% and 70% lower, respectively, than the mean values, both with and without ketoconazole coadministration. Thus, the interaction did not differ significantly from the mean value, suggesting that complete inhibition was still obtained. In fasted condition,  $F$  was found to be 3.9% (90% CI = 3.06–5.02) in Study 3 (de Vries et al. 2015), implying that a 24-fold increase in ibrutinib  $AUC_{\infty}$  with ketoconazole (Study 1 and hence a different cohort of participants) would result in  $F$  of approximately 73–121% (24 9 3.06 to 5.02%). In line with ketoconazole study observations, intersubject variability of ibrutinib exposure increased following rifampin coadministration, due to significantly decreased bioavailability.

When ibrutinib was given with ketoconazole and rifampin at the same time, the concentration of the metabolite PCI-45227 dropped. The possible explanation for the reduced exposure of PCI-45227 to rifampin might be the increased metabolism of PCI-45227 by CYP3A or the stimulation of P-gp, a protein that PCI-45227 is a substrate for. Research conducted by Bjorkhem-Bergman et al. (2013), Marde Arrhen et al. (2013), and Dutreix et al. (2014) found that a rise in 4-b-hydroxycholesterol, an endogenous biomarker of CYP3A activity, was

associated with reductions in  $C_{max}$  and AUC in Study 2. Consistent with earlier findings, these findings were published in 2013 by Bjorkhem-Bergman et al.

The results of trials 1 and 2 show that ibrutinib is metabolized nearly entirely by CYP3A throughout its first journey through the intestines and liver. The previous in silico PBPK simulations (unpublished) demonstrated a 10- and 11-fold reduction (GMR) in simulated ibrutinib AUC and  $C_{max}$ , respectively, after 600 mg q.d. of rifampin. The present study's

results corroborated these findings. In a similar vein, the outcomes were in agreement with the predicted ketoconazole interaction. It is advised to refrain from using powerful CYP3A inhibitors and inducers at the same time to prevent ibrutinib over-and under-exposures, respectively, as has been seen with other sensitive CYP3A substrates.

Guo et al. (2000) and Guo and Yamazoe (2004) demonstrated that furanocoumarins in GFJ are strong CYP3A inhibitors in humans, which may lead to interactions between GFJ and drugs in the digestive tract. In order to distinguish between the first-pass effects in the intestinal wall and the liver, single-strength (250 mL) GFJ was given at various times prior to ibrutinib dose in Study 3. Multiple studies have shown that inhibiting mucosal metabolism increases bioavailability and decreases first-pass metabolism (Bailey et al., 1995; Ducharme et al., 1995; Veronese et al., 2003; Seidegard et al., 2012).

There was a 50% reduction in apparent clearance and an increase in ibrutinib concentrations after pretreatment with GFJ. Nonetheless, there was no difference in intravenous clearance. This lines up with previous pharmacokinetic studies that used GFJ, such as those by Garg et al. (1998), Hanley et al. (2011), and Shoaf et al. (2012). After first-pass metabolism in the stomach, around 47% of ibrutinib is accessible under nonfasted conditions, according to a comparison of the F of ibrutinib with and without GFJ. The liver processes the vast majority of this quantity (de Vries et al. 2015).

It was previously shown that ibrutinib may have a notable impact on food digestion (de Jong et al. 2014). When given when fasting, ibrutinib had an AUClast of around 60% of what it would have been 30 minutes before or 2 hours after a meal. Another research that showed full oral absorption of ibrutinib was a mass-balance investigation done while the subjects were fasting (Scheers et al. 2015). The result of this is the

theory that suggests that food enhances oral bioavailability via decreasing hepatic and intestinal CYP3A first-pass elimination instead than via lipid-assisted solubilization. In summary, compared to a fasted state, food increases the flow of blood through the mesenteric and splanchnic veins, which shortens the amount of time a drug spends in the gastrointestinal tract and liver. This, in turn, shortens the amount of time the drug spends in central circulation, leading to higher systemic bioavailability. Budesonide and other medications

with a high extraction rate were shown to have a similar pattern (Marasanapalle et al. 2011; Seidegard et al. 2012). Consequently, the GFJ-induced DDI on ibrutinib AUC in this research is lower than the projected value in the following fasting scenario. In order to enable DDI simulations in the presence of food, these data were then used to enhance the PBPK model [unpublished].

The first research used ibrutinib doses of 120 mg when taken alone and 40 mg when used with ketoconazole in order to reduce drug exposure. Since Study 1 was the first to include healthy participants and because it was assumed that ibrutinib exposure would rise after ketoconazole treatment, a reduced dosage of 40 mg of ibrutinib was selected as a safety precaution. Additionally, PK non-linearity was not suspected. Study 2 used therapeutic levels of ibrutinib since its effects in Study 1 were well-tolerated and the exposures patients experienced were higher than the mean exposures at 560 mg. In Study 3, a 140 mg dosage of ibrutinib was employed instead of a 560 mg dose to account for the possible effect of GFJ-induced CYP3A inhibition at the level of intestinal lumen absorption. The maximum increase in exposure due to GFJ would not be more than fourfold, according to simulations conducted using SimCyp® modeling and simulation software. Consequently, the exposures would not be higher than those in the 560 mg treatment. The maximum recommended daily dosages for ketoconazole and rifampin, respectively, are 400 mg and 600 mg, respectively.

Regardless of meal or GFJ consumption status, all three treatments were well-tolerated, and no treatment-emergent adverse events persisted. It should be mentioned, nevertheless, that these studies used healthy volunteers; it is necessary to determine the level of interaction in a medical environment, when individuals may be exposed to multiple medications.

In conclusion, ibrutinib's exposure was higher when administered in conjunction with GFJ and ketoconazole, two strong and moderate CYP3A inhibitors, and lower when administered in conjunction with rifampin, a strong CYP3A inducer. While rifampin raised the mean metabolite to parent ratio, ketoconazole and GFJ lowered it after coadministration with CYP3A inhibitors. The level of ibrutinib exposure that increased with the level of CYP3A inhibition was

increased in subjects with lower area under the curve (AUC) and greater baseline clearance, most likely due to higher CYP3A expression in such subjects to

begin with. As a result, it follows that individuals with a high baseline exposure would not experience significant increases while taking powerful inhibitors concurrently, as the bioavailability of these drugs cannot be exceeded. We did not notice any new safety signals. When treating a patient on ibrutinib, it is necessary to interrupt or modify the dosage if strong or moderate CYP3A inhibitors are to be administered. In individuals using two CYP3A inhibitors at the same time, pharmacokinetic and safety data are still being collected. Patients who received ibrutinib concurrently with moderate or mild CYP3A inhibitors seemed to have an exposure that was within twice the upper limit of the exposure seen in patients who did not take CYP3A inhibitors, according to uncontrolled clinical trials with small and unequal sample group size. Sukbuntherng et al. (2014) propose to validate the interaction potential in a patient group with a cancer diagnosis by conducting a DDI trial of ibrutinib with CYP3A inhibitors.

#### References

In 2013, the authors were Advani RH, Buggy JJ, Sharman JP, Smith SM, Boyd TE, Grant B, and others. Patients with B-cell malignancies who have relapsed or are resistant to previous treatments show substantial improvement when given the bruton tyrosine kinase inhibitor ibrutinib (PCI-32765). *American Journal of Clinical Oncology*, 31(1), pp. 88–94.

It was published in 1995 by Bailey DG, Arnold JM, Bend JR, Tran LT, and Spence JD. Reproducibility and characterisation of the grapefruit juice-felodipine interaction using the extended release medication formulation. *Br The citation is from the Journal of Clinical Pharmacology*, volume forty, pages 135–140.

As a group, Bjorkhem-Bergman, Backstrom, Nylen, Ronquist-Nii, Bredberg, Andersson, and others published a study in 2013. Assessing the effects of rifampicin on CYP3A4 induction using midazolam and endogenous 4-hydroxycholesterol as indicators. *Medications Metab Disposal* 41: 1488-1493.

In 2013, Byrd JC, Furman RR, Coutre SE, Flinn IW, Burger JA, Blum KA, and others published. Relapsed chronic lymphocytic leukemia: ibrutinib targeting BTK. *Journal of the National Academies of Medicine* 369: 32-42.

In 1995, Ducharme, Warbasse, and Edwards published a paper. Grapefruit juice and the elimination of cyclosporine from the body following

intravenous and oral treatment. Pages 485–491 in *Clin Pharmacol Ther* 57.

Published in 2014 by Dutreix, Lorenzo, and Wang. Using midostaurin and rifampicin as drug-drug interaction indicators, we compared two endogenous biomarkers of CYP3A4 activity. *Eur J Clinical pharmacology*, volume 70, pages 915–920.

Published in 2004 by Fuentes-Panana EM, Bannish G, and Monroe JG. The control mechanisms and function of basal B-cell receptor signaling in B lymphocytes: applications in positive selection, differentiation, and peripheral survival. *Review of Immunology* 197: 26–40.

A study conducted by Garg SK, Kumar N, Bhargava VK, and Prabhakar SK in 1998. The impact of grapefruit juice on the bioavailability of carbamazepine in epileptic individuals. The journal *clinical pharmacology and therapeutics* published an article with the DOI: (64).

Researchers Guo and Yamazoe (2004) found that grapefruit juice and herbal remedies included furanocoumarins, which inhibited cytochrome P450. The article is published in *Acta Pharmacol Sin* 25: 129-136.

Yukazuke Y, Guo LQ, Taniguchi M, Xiao YQ, Baba K, Ohta T, and Yamazoe L (2000). The impact of naturally occurring furanocoumarins on the activity of human microsomal cytochrome P450 3A. Publication: *Jpn J Pharmacol* 82: 122-129.

In 2011, Hanley MJ, Cancalon P, Widmer WW, and Greenblatt DJ published on the subject. Grapefruit juice's impact on medication elimination. *Clinical Pharmacology and Toxicology: Expert Opinion* 7: 267-286.

According to a study by Honigberg LA, Smith AM, Sirisawad M, Verner E, Loury D, Chang B, and others (2010). In autoimmune illness and B-cell cancer models, the Bruton tyrosine kinase inhibitor PCI-32765 effectively prevents B-cell activation. The process Publication: *National Academy of Sciences, USA*, 107: 13075-13080.

2014. Imbruvica™. Overview of the product The Agency for Medicines in Europe. Check it out at <http://>

in 2015, the authors were de Jong, Sukbuntherng, Skee, Murphy, O'Brien, Byrd, and ourselves. Pharmacokinetics of oral ibrutinib in healthy individuals and those with chronic lymphocytic leukemia as a function of diet. *Cancer "Chemistry and Pharmacology"* 75: 907-916.

In a 2014 study, Sukbuntherng et al. collected data

from a variety of sources. Assessment of the safety and pharmacokinetics of ibrutinib in individuals with B-cell malignancies using CYP3A inhibitors simultaneously. Held in Austin, Texas, from October 12th to the 15th, during the annual conference of the American College of Clinical Pharmacy (ACCP).

In 2005, Kuppers R. What causes B-cell lymphoma? *Journal of the National Cancer Institute*, 5(3), 251-262.

Tang F., Zhu H., Grill A., Boinpally RR., Marasanapalle VP. (2011). Food and medication interactions and their effects on systemic clearance. The authors of the 2013 study were Marde Arrhen Y, Nylen H, Lovgren-Sandblom A, Kanebratt KP, Wide K, and Diczfalusy U. As indicators of CYP3A4 induction, 4beta-hydroxycholesterol (cholesterol) and 6beta-hydroxycortisol (cortisol) are compared. The citation for this article is *Br J Clin Pharmacol* 75: 1536-1540.

Researchers Marostica, Sukbuntherng, Loury, de Jong, de Trixhe, Vermeulen, and colleagues (2015). Bruton tyrosine kinase inhibitor ibrutinib population pharmacokinetic model in B cell cancer patients. *Cancer The chemical pharmacology journal articles* are cited as: 75: 111-121.

In 2014, Parmar, Patel, and Pinilla-Ibarz published a paper. A new targeted treatment for chronic lymphocytic leukemia called ibrutinib (imbruvica). *Phys. Rev.* 39: 483-519.

2015, de Vries et al. conducted a study on the effects of grapefruit juice on ibrutinib and the stability of isotope-intravenous microdoses for absolute bioavailability in healthy adults. *The British Journal of Clinical Pharmacology* is about to publish an article.

In 2015, a group of researchers including Scheers, Leclercq, de Jong, Bode, Bockx, Laenen, and others published a paper. Oral <sup>14</sup>C-radiated ibrutinib metabolism, absorption, and excretion: a one-dose, open-label, phase I trial in healthy males. *Medicines Disposal* 43: 289-297.

Authors: Seidegard, Nyberg, and Borga (2012). Local pretreatment with escalating dosages of ketoconazole in the proximal jejunum to differentiate budesonide metabolism by the mucosa and the liver. *European Journal of Pharmaceutical Science*, 46, 530-536.

In 2012, Shoaf, Mallikaarjun, and Bricmont published a study. Tolvaptan is a non-peptide arginine vasopressin antagonist; in healthy individuals, the effect of grapefruit juice on its pharmacokinetics is studied. Publication: *European Journal of Clinical Pharmacology*, Volume 68, Pages 207-211.

Authors: Veronese ML, Gillen LP, Burke JP, Dorval EP, Hauck WW, Pequignot E, and others (2003). Grapefruit juice inhibits hepatic and intestine CYP3A4 in vivo in a dose-dependent manner. *Clinical pharmacology*, volume 43, pages 831-839, 2014.